Supporting Information

Implications of Crystallization Temperatures of Organic Small Molecules in Optimizing Nonfullerene Solar Cell Performance

Xiafei Cheng[a], Miaomiao Li[a, *], Ziqi Liang[a], Mengyuan Gao[a], Long Ye [a, *], Yanhou Geng [a, b, *]

[a] School of Materials Science and Engineering, and Tianjin Key Laboratory of Molecular Optoelectronic Science, Tianjin University, Tianjin, 300072, China

[b] Joint School of National University of Singapore and Tianjin University, International Campus of Tianjin University, Binhai New City, Fuzhou 350207, China

*Corresponding authors

E-mail: miaomiao.li@tju.edu.cn; yelong@tju.edu.cn; yanhou.geng@tju.edu.cn.

1. Materials and Synthesis

All chemical raw materials were purchased from commercial sources and used without further purification. Anhydrous chloroform (CF) was purchased from Sigma-Aldrich. N3 and Y6 were purchased from Y6 Sale (Shenzhen), and PDINO was purchased from Derthon Optoelectronic Materials Science Technology Co., Ltd, respectively. DRTT-R and DRTT-T were synthesized in our lab according to our previous work[1]. DRTT-2T and DRTT-TT were synthesized and used for comparison. The synthetic route to DRTT-2T and DRTT-TT is shown in Scheme S1. Organotin monomers (5-(2-ethylhexyl)thieno[3,2-b]thiophen-2-yl)trimethylstannane (**1a**), (5-(2-ethylhexyl)thieno[3,2-b]thiophen-2-yl)trimethylstannane (**1b**) and 6-bromo-4,8-bis(5-(2-ethylhexyl)thiophen-2-yl)benzo[1,2-b:4,5-b']dithiophene-2-carbaldehyde (**4**) were synthesized according to the literature[2-4].

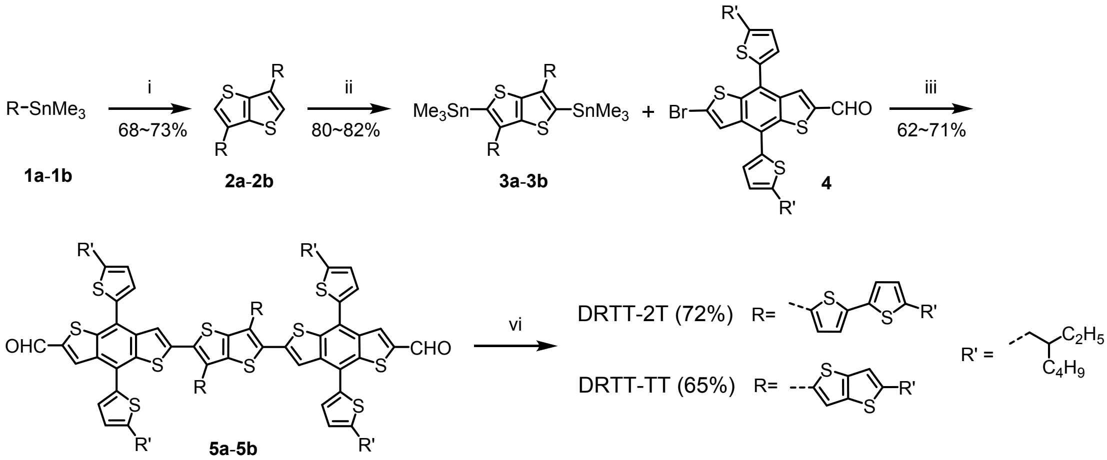

Scheme S1. Synthetic route to DRTT-2T and DRTT-TT.

3,6-bis(5'-(2-ethylhexyl)-[2,2'-bithiophen]-5-yl)thieno[3,2-b]thiophene (**2a**). To a reaction tube were added compound **1a** (2.5 g, 4.8 mmol), 3,6-dibromothieno[3,2-b]thiophene (574.1 mg, 1.9 mmol), $Pd(PPh_3)_4$ (178.1 mg, 154.1 μmol) and anhydrous toluene (4.0 mL) in glove box. The mixture was stirred in a microwave reactor at a dynamic model (160 ^{o}C, 200 W) for 1 hour. Then the reaction mixture was poured into water and extracted with CH_2Cl_2. The combined organic extracts were dried over anhydrous $MgSO_4$. After evaporating the solvent, the residue was purified by column chromatography on silica gel with hexane as eluent to afford the product as a light yellow solid (0.8 g, 68%). ^{1}H NMR ($CDCl_3$, 400 MHz): δ (ppm) = 7.50 (s, 2H), 7.27 (d, 2H), 7.10 (d, 2H), 7.04 (d, 2H), 6.68 (d, 2H), 2.75 (d, 4H), 1.60 (m, 2H), 1.38-1.35 (m, 16 H), 0.93-0.89 (m, 12H). ^{13}C NMR (100 MHz, $CDCl_3$): δ (ppm) = 144.37, 137.27, 137.16, 135.10, 134.63, 128.25, 125.93, 124.70, 123.52, 123.46, 121.50, 41.43, 34.17, 32.39, 28.89, 25.53, 23.02, 14.15, 10.85. MS (MALDI-TOF) *m/z*: calcd. for $C_{38}H_{44}S_6$: 692.2; Found. 691.2.

5,5''-bis(2-ethylhexyl)-2,3':6',2''-terthieno[3,2-b]thiophene (**2b**). **2b** (0.9 g, 73%) was obtained as a light yellow solid from **1b** (2.0 g, 4.5 mmol) following the procedure for the synthesis of **2a**. ^{1}H NMR ($CDCl_3$, 400 MHz): δ (ppm) = 7.53 (s, 2H), 7.48 (s, 2H), 6.94 (s, 2H), 2.85 (d, 4H), 1.65 (m, 2H), 1.42-1.31 (m, 16H), 0.94-0.89 (m, 12H). ^{13}C NMR (100 MHz, $CDCl_3$): δ (ppm) = 147.70, 137.94, 137.52, 137.32, 136.91, 129.04, 121.46, 117.27, 116.49, 41.44, 35.26, 32.39, 28.88, 25.52, 23.02, 14.16, 10.82. MS (MALDI-TOF) *m/z*: calcd. for $C_{34}H_{40}S_6$: 640.2; Found. 639.2.

(3,6-bis(5'-(2-ethylhexyl)-[2,2'-bithiophen]-5-yl)thieno[3,2-b]thiophene-2,5-diyl)bis(trimethylstannane) (**3a**). Under the protection of argon, *t*-butyllithium (1.3 M, 0.7 ml, 952.2 μmol) was dropwise added to compound **2a** (300.0 mg, 432.8 μmol) in dry THF (15 ml) at -78 °C. After stirring for 2 h, the mixture was warmed to room temperature and stirred for 1 h. Then Me_3SnCl (1M, 1.0 ml, 1.0 mmol) was added into the mixture at -78 °C, and then the mixture was warmed to room temperature and stirred for 12 h. Subsequently, the mixture was poured into saturated KF aqueous solution and extracted with CH_2Cl_2. The organic layer was washed with water and dried over anhydrous $MgSO_4$ and concentrated to afford compound **3a** (352.7 mg, 80%), which was used for the next step without purification. ^{1}H NMR ($CDCl_3$, 400 MHz): δ (ppm) = 7.11 (d, 4H), 7.04 (d, 2H), 6.69 (d, 2H), 2.76 (d, 4H), 1.60 (m, 2H), 1.38-1.35 (m, 16 H), 0.93-0.89 (m, 12H), 0.38 (s, 18H).

(5,5''-bis(2-ethylhexyl)-[2,3':6',2''-terthieno[3,2-b]thiophene]-2',5'-diyl)bis(trimethylstannane) (**3b**). **3b** (371.0 mg, 82%) was obtained from **2b** (300.0 mg, 468.0 μmol) following the procedure for the synthesis of **3a**. ^{1}H NMR ($CDCl_3$, 400 MHz): δ (ppm) = 7.33 (s, 2H), 6.94 (s, 2H), 2.85 (d, 4H), 1.65 (m, 2H), 1.38-1.35 (m, 16 H), 0.93-0.89 (m, 12H), 0.36 (s, 18H).

6,6'-(3,6-bis(5'-(2-ethylhexyl)-[2,2'-bithiophen]-5-yl)thieno[3,2-b]thiophene-2,5-diyl)bis(4,8-bis(5-(2-ethylhexyl)thiophen-2-yl)benzo[1,2-b:4,5-b']dithiophene-2-carbaldehyde) (**5a**). To a reaction tube were added compound **3a** (420.0 mg, 412.3 μmol), **4** (621.5 mg, 907.2 μmol), $Pd(PPh_3)_4$ (38.1 mg, 33.0 μmol) and anhydrous toluene (9.0 mL) in glove box. The mixture was stirred in a microwave reactor at a dynamic model (170 ^{o}C, 200 W) for 1 hour. Then the solvent was evaporated, the residue was purified by column chromatography on silica gel with $CHCl_3$ as eluent to afford the product as a red solid (557.6 mg, 71%). ^{1}H NMR ($CDCl_3$, 400 MHz): δ (ppm) = 10.02 (s, 2H), 8.31 (s, 2H), 7.76 (s, 2H), 7.30 (d, 2H), 7.22 (d, 2H), 7.20 (d, 2H), 7.09 (d, 2H), 7.02

(d, 2H), 6.89 (d, 2H), 6.76 (d, 2H), 6.67 (d, 2H), 2.86 (d, 4H), 2.75 (d, 8H), 1.70 (m, 2H), 1.64 (m, 4H), 1.43-1.30 (m, 48H), 0.95-0.88 (m, 36H). ^{13}C NMR (100 MHz, $CDCl_3$): δ (ppm) = 184.50, 146.82, 146.50, 144.57, 143.35, 141.22, 139.99, 139.58, 139.43, 139.31, 138.74, 135.67, 135.53, 134.54, 134.37, 133.67, 132.23, 129.01, 128.41, 126.45, 125.99, 125.74, 125.51, 125.30, 124.67, 123.95, 123.12, 41.43, 41.42, 41.34, 34.24, 34.21, 34.18, 32.48, 32.43, 32.41, 28.89, 25.71, 25.62, 25.51, 23.06, 23.03, 14.18, 14.16, 10.88, 10.83. MS (MALDI-TOF) *m/z*: calcd. for $C_{108}H_{124}O_2S_{14}$: 1901.6; Found. 1900.5. Elemental Anal. Calcd.: C, 68.16; H, 6.57; O, 1.68; S, 23.59; Found. C, 68.13; H, 6.41; S, 23.73.

6,6'-(5,5''-bis(2-ethylhexyl)-[2,3':6',2''-terthieno[3,2-b]thiophene]-2',5'-diyl)bis(4,8-bis (5-(2-ethylhexyl)thiophen-2-yl)benzo[1,2-b:4,5-b']dithiophene-2-carbaldehyde) (**5b**). **5b** (556.6 mg, 62%) was obtained as a red solid from **3b** (470.0 mg, 484.1 μmol) following the procedure for the synthesis of **5a**. ^{1}H NMR ($CDCl_3$, 400 MHz): δ (ppm) = 10.03 (s, 2H), 8.31 (s, 2H), 7.74 (s, 2H), 7.41 (s, 2H), 7.27 (d, 2H), 7.11 (d, 2H), 6.94 (s, 2H), 6.87 (d, 2H), 6.70 (d, 2H), 2.88-2.83 (m, 8H), 2.77 (d, 4H), 1.70-1.61 (m, 6H), 1.44-1.32 (m, 48H), 0.96-0.90 (m, 36H). ^{13}C NMR (100 MHz, $CDCl_3$): δ (ppm) = 184.45, 148.06, 146.75, 146.37, 143.31, 141.10, 140.11, 139.67, 139.43, 139.19, 138.64, 137.65, 135.65, 135.62, 135.53, 134.50, 133.93, 128.50, 128.40, 126.40, 125.69, 125.38, 124.64, 120.49, 117.38, 41.47, 41.40, 35.30, 34.26, 32.49, 32.44, 29.72, 28.91, 25.71, 25.66, 25.47, 23.06, 23.04, 14.19, 14.17, 10.88, 10.80. MS (MALDI-TOF) *m/z*: calcd. for $C_{104}H_{120}O_2S_{14}$: 1849.5; Found. 1848.5. Elemental Anal. Calcd.: C, 67.49; H, 6.54; O, 1.73; S, 24.25; Found. C, 67.36; H, 6.38; S, 24.43.

DRTT-2T. A solution of compound **5a** (300 mg, 157.6 μmol) and 3-ethyl-2-thioxothiazolidin-4-one (254.2 mg, 1.6 mmol) in dry $CHCl_3$ (16 mL) was degassed twice with argon followed by the addition of a few drops of triethylamine. Then the reaction mixture was stirred at 70 °C for 8 hours. The solvent was removed under reduced pressure and the residues were purified by column chromatography on silica gel with $CHCl_3$ as eluent and Concentrated to a saturated solution then added dropwise in methanol for precipitation. The solid was collected by filtration to afford the product as a dark red solid (248.4 mg, 72%). ^{1}H NMR ($CDCl_3$, 400 MHz): δ (ppm) = 7.80 (s, 2H), 7.76 (s, 2H), 7.62 (s, 2H), 7.24 (d, 2H), 7.19 (d, 2H), 7.08 (d, 2H), 7.07 (d, 2H), 7.00 (d, 2H), 6.84 (d, 2H), 6.78 (d, 2H), 6.69 (d, 2H), 4.15 (q, 4H), 2.85 (d, 4H), 2.78 (m, 8H), 1.71-1.62 (m, 6H), 1.45-1.40 (m, 48H), 1.25 (t, 6H), 0.98-0.92 (m, 36H). ^{13}C NMR (100 MHz, $CDCl_3$): δ (ppm) = 192.24, 166.97, 146.52, 146.39, 144.44, 141.35, 140.08, 139.51, 138.05, 137.97, 137.86, 135.98, 135.93, 134.47, 134.01, 132.27, 128.53, 128.42, 126.01, 125.64, 125.55, 123.97, 123.29, 123.11, 41.44, 41.40, 41.32, 34.31, 34.25, 34.20, 32.51, 32.45, 28.95, 28.92, 25.69, 25.53, 23.13, 23.08, 23.05, 14.25, 14.22, 14.19, 12.30, 10.94, 10.89 10.84. MS (MALDI-TOF) *m/z*: calcd. for $C_{118}H_{134}N_2O_2S_{18}$: 2187.6; Found. 2186.5. Elemental Anal. Calcd.: C, 64.73; H, 6.17; N, 1.28; O, 1.46; S, 26.36; Found. C, 64.57; H, 6.01; N, 1.37; S, 26.59.

DRTT-TT. DRTT-TT (224.3 mg, 65%) was obtained as a dark red solid from **5b** (300 mg, 162.1 μmol) and 3-ethyl-2-thioxothiazolidin-4-one (261.3 mg, 1.6 mmol) following the procedure for the synthesis of DRTT-2T. ^{1}H NMR ($CDCl_3$, 400 MHz): δ (ppm) = 7.78 (s, 2H), 7.74 (s, 2H), 7.57 (s, 2H), 7.11 (d, 2H), 7.09 (d, 2H), 6.95 (s, 2H), 6.81 (d, 2H), 6.69 (d, 2H), 4.13 (q, 4H), 2.93 (m, 4H), 2.86 (m, 8H), 1.73-1.68 (m, 6H), 1.74-1.30 (m, 48H), 1.24 (t, 6H), 1.00-0.87 (m, 36H). ^{13}C NMR (100 MHz, $CDCl_3$): δ (ppm) = 192.22, 166.94, 147.84, 146.44, 146.29, 141.19, 140.18, 139.69, 139.32, 137.90, 137.85, 137.81, 137.63, 136.00, 135.93, 135.88, 134.34, 131.66, 128.64, 128.40, 125.59, 125.38, 124.98, 117.44, 41.52, 41.39, 39.83, 35.32, 34.37, 34.28, 32.56, 32.53, 32.48, 29.00, 28.96, 28.93, 25.76, 25.68, 25.46, 23.10, 14.23, 14.20, 12.30, 11.00, 10.89, 10.82. MS (MALDI-TOF) *m/z*: calcd. for $C_{114}H_{130}N_2O_2S_{18}$: 2135.5; Found. 2134.5. Elemental Anal. Calcd.: C, 64.06; H, 6.13; N, 1.31; O, 1.50; S, 27.00; Found. C, 63.89; H, 5.98; N, 1.39; S, 27.21.

2. Instruments

UV-vis-NIR absorption spectra were obtained on a Shimadzu UV3600-plus spectrometer. Solution spectra were measured in CF with a concentration of 1×10^{-5} mol L^{-1} and films were prepared by spin-casting with CF as solvent. Optical bandgaps were calculated according to absorption onsets of the neat films (E_g^{opt} = 1240/λ_{onset} eV). Cyclic voltammetry (CV) measurements were carried out on a CHI660a electrochemical workstation at a scan rate of 100 mV s^{-1}. A glassy carbon with 1 cm diameter, a Pt wire and a saturated calomel electrode (SCE) were used as working electrode, counter electrode and reference electrode, respectively. NBu_4PF_6 (0.1 M) in anhydrous acetonitrile was used as electrolyte. The potential was calibrated by ferrocene/ferrocenium (Fc/Fc^+). The HOMO and LUMO energy levels were estimated by the equations: E_{HOMO} = -(4.80 + $E_{\mathrm{onset}}^{\mathrm{ox}}$) eV and E_{LUMO} = -(4.80+$E_{\mathrm{onset}}^{\mathrm{re}}$) eV, in which $E_{\mathrm{onset}}^{\mathrm{ox}}$ and $E_{\mathrm{onset}}^{\mathrm{re}}$ are oxidation and reduction onsets versus the half potential of Fc/Fc^+, respectively. Differential scanning calorimetry (DSC) was conducted on a Q25 differential scanning calorimeter (TA Instruments) with a heating/cooling rate of

10 ^{o}C min^{-1} under nitrogen. Out of plane GIWAXS of the thin films were measured by a Rigaku Smart Lab with Cu K_{α} source (λ = 1.54056 Å) in air. TEM images were acquired on a JEM-2100PLUS electron microscopy (JEOL) at a 200 kV accelerating voltage. Keithley 2400 source meter was used to measure *J-V* curves under 100 mW cm^{-2} AM 1.5G simulated solar light illumination provided by a Solar Simulator (SS-F5-3A, Enli Technology Co. Ltd) calibrated with a standard photovoltaic cell equipped with a KG5 filter in a glove box. The EQE curves were recorded by the integrated quantum efficiency measurement system QE-R (Enli Technology Co. Ltd., Taiwan), which was calibrated with a crystal silicon photovoltaic cell ahead of the measurement.

3. SCLC Measurement

The hole/electron mobility was measured using the space charge limited current (SCLC) method. Hole-only and electron-only devices were fabricated with architecture of ITO/PEDOT:PSS (35 nm)/active layer (100 nm)/Au (100 nm) and ITO/ZnO (30 nm)/active layer (100 nm)/Al (100 nm), respectively. The devices were measured using Keithley 2400 source meter in the dark and the mobilities were obtained by taking current-voltage curves and fitting the results to a space charge limited form, where the SCLC is described by:

$$J = \frac{9}{8}\varepsilon_0\varepsilon_r\mu\frac{V^2}{L^3}$$

Where J is the current density, L is the thickness of the film, μ is the hole or electron mobility, ε_0 is the permittivity of free space, ε_r is the relative permittivity of the material (assumed to be 3), V (= V_{appl} - V_{bi}) is the internal voltage in the device, where V_{appl} is the applied voltage, V_{bi} is the built-in voltage (0 V), V_{rs} is the voltage drop from the substrate's series resistance (V_{rs} = IR, R is measured to be 10.8 Ω).

4. Supplementary Data

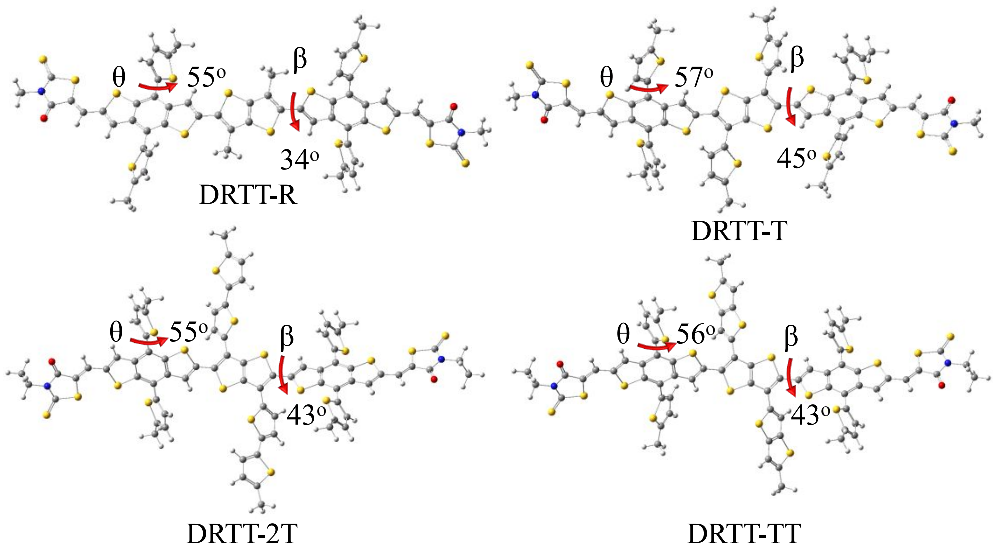

Figure S1. DFT optimized molecular geometries of DRTT-R, DRTT-T, DRTT-2T and DRTT-TT. All alkyl substituents were replaced with methyl groups for simplifying the calculations.

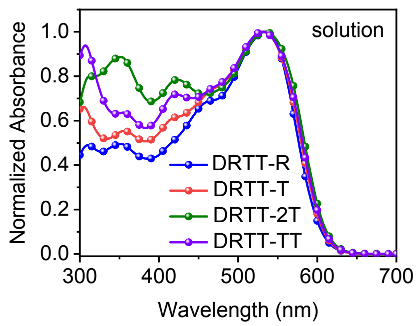

Figure S2. Absorption spectra of the molecules in chloroform solutions (10^{-5} mol/L in chloroform).

Table S1. Out-of-plane XRD data of DRTT-R neat films without and with thermal annealing.

TA temperature (°C)	(100)					(010)				
	q (Å^{-1})	d-spacing (Å)	FWHM Δq (Å^{-1})	CCL (Å)	Area	q (Å^{-1})	d-spacing (Å)	FWHM Δq (Å^{-1})	CCL (Å)	Area
No	0.34	18.47	0.049	128.16	721	N/A	N/A	N/A	N/A	N/A
40	0.35	17.94	0.042	135.54	802	N/A	N/A	N/A	N/A	N/A
50	0.35	17.94	0.041	136.85	1106	N/A	N/A	N/A	N/A	N/A
60	0.35	17.94	0.041	137.85	1246	N/A	N/A	N/A	N/A	N/A
70	0.34	18.47	0.038	150.72	1306	N/A	N/A	N/A	N/A	N/A
80	0.34	18.47	0.034	166.24	1364	1.76	3.57	0.180	31.40	15
90	0.34	18.47	0.033	171.27	2079	1.80	3.49	0.100	56.52	11
100	0.34	18.47	0.033	171.27	2299	1.81	3.46	0.112	50.54	15
110	0.34	18.47	0.032	176.63	2648	1.82	3.45	0.110	51.38	14
120	0.33	19.03	0.031	182.32	3274	1.82	3.45	0.100	56.52	15

[a] N/A denotes not available.

Table S2. Out-of-plane XRD data of DRTT-T neat films without and with thermal annealing.

TA temperature (°C)	(100)					(010)				
	q (Å^{-1})	d-spacing (Å)	FWHM Δq (Å^{-1})	CCL (Å)	Area	q (Å^{-1})	d-spacing (Å)	FWHM Δq (Å^{-1})	CCL (Å)	Area
No	0.32	19.63	0.094	60.13	46	N/A	N/A	N/A	N/A	N/A
40	0.32	19.63	0.085	66.50	93	N/A	N/A	N/A	N/A	N/A
50	0.32	19.63	0.059	95.76	199	N/A	N/A	N/A	N/A	N/A
60	0.31	20.26	0.038	150.72	1211	1.72	3.65	0.150	37.68	48
70	0.31	20.26	0.037	152.76	1227	1.73	3.63	0.140	40.37	78
80	0.31	20.26	0.031	182.32	1502	1.73	3.63	0.120	47.10	64
90	0.31	20.26	0.027	209.33	1620	1.74	3.61	0.120	47.10	64
100	0.31	20.26	0.025	226.08	2688	N/A	N/A	N/A	N/A	N/A
110	0.31	20.26	0.026	221.39	4272	N/A	N/A	N/A	N/A	N/A

[a] N/A denotes not available.

Table S3. Out-of-plane XRD data of DRTT-2T neat films without and with thermal annealing.

TA temperature (^{o}C)	(100)					(010)				
	q (Å^{-1})	d-spacing (Å)	FWHM Δq (Å^{-1})	CCL (Å)	Area	q (Å^{-1})	d-spacing (Å)	FWHM Δq (Å^{-1})	CCL (Å)	Area
No	0.28	22.43	0.086	65.72	22	N/A	N/A	N/A	N/A	N/A
40	0.28	22.43	0.089	63.51	112	N/A	N/A	N/A	N/A	N/A
50	0.27	23.26	0.086	65.72	141	N/A	N/A	N/A	N/A	N/A
60	0.27	23.26	0.068	83.12	212	N/A	N/A	N/A	N/A	N/A
70	0.27	23.26	0.052	108.69	442	1.67	3.76	0.230	24.57	65
80	0.28	22.43	0.047	120.26	823	1.70	3.69	0.130	43.48	52
90	0.28	22.43	0.045	125.60	845	1.71	3.67	0.130	43.48	68
100	0.27	23.26	0.043	131.44	1216	1.71	3.67	0.110	51.38	78
110	0.28	22.43	0.041	137.85	1629	1.71	3.67	0.120	47.10	81
120	0.27	23.26	0.040	141.30	1801	1.72	3.65	0.090	62.80	88

[a] N/A denotes not available.

Table S4. Out-of-plane XRD data of DRTT-TT neat films without and with thermal annealing.

TA temperature (^{o}C)	(100)					(010)				
	q (Å^{-1})	d-spacing (Å)	FWHM Δq (Å^{-1})	CCL (Å)	Area	q (Å^{-1})	d-spacing (Å)	FWHM Δq (Å^{-1})	CCL (Å)	Area
No	0.31	20.26	0.099	56.90	22	N/A	N/A	N/A	N/A	N/A
50	0.32	19.63	0.099	57.10	61	N/A	N/A	N/A	N/A	N/A
60	0.32	19.63	0.100	56.40	136	N/A	N/A	N/A	N/A	N/A
70	0.31	20.26	0.098	57.50	148	N/A	N/A	N/A	N/A	N/A
80	0.30	20.93	0.068	83.20	170	N/A	N/A	N/A	N/A	N/A
90	0.30	20.93	0.054	104.70	179	N/A	N/A	N/A	N/A	N/A
100	0.29	21.66	0.041	137.90	1200	1.70	3.69	0.150	37.68	117
110	0.29	21.66	0.033	171.30	2291	1.71	3.67	0.100	56.52	135
120	0.29	21.66	0.028	201.90	4526	1.71	3.67	0.120	47.10	141

[a] N/A denotes not available.

Figure S2. DFT optimized molecular geometries of DRTT-R, DRTT-T, DRTT-2T and DRTT-TT. All alkyl substituents were replaced with methyl groups for simplifying the calculations.

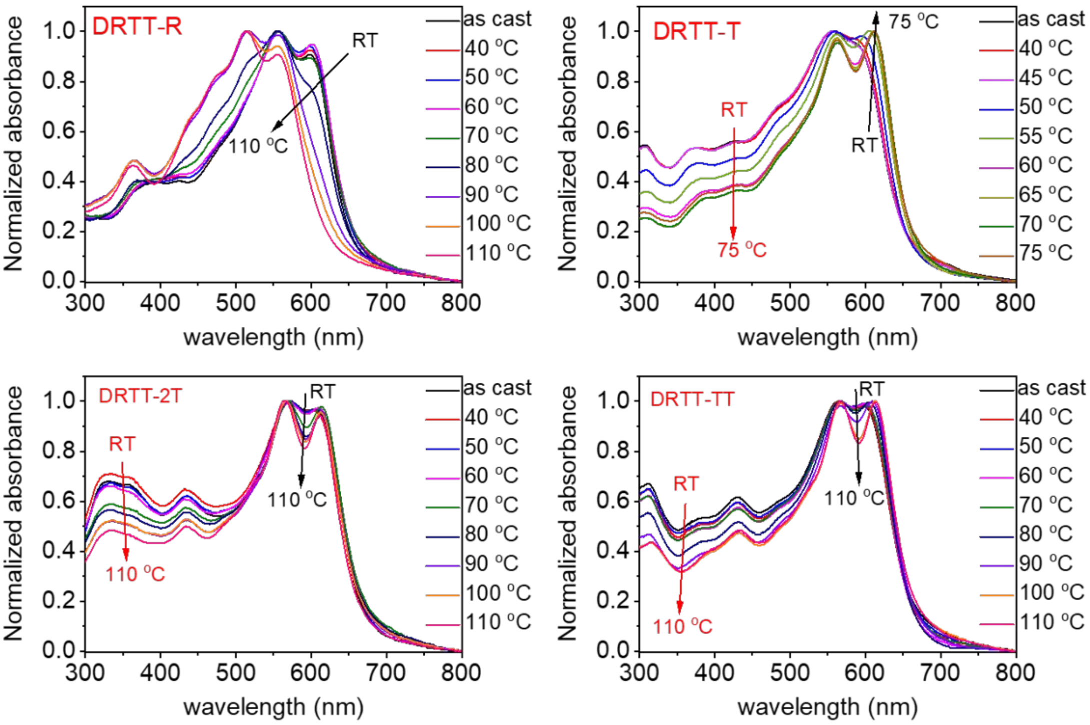

Figure S3. Normalized UV-vis absorption spectra of DRTT-R, DRTT-T, DRTT-2T and DRTT-TT neat films without and with thermal annealing.

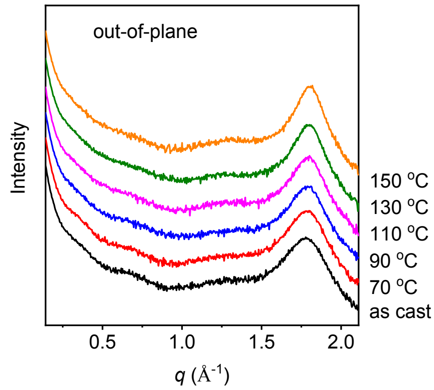

Figure S4. Out-of-plane XRD patterns of N3 neat films without and with thermal annealing.

Table S5. (100) diffraction data in out-of-plane direction of DRTT-R:N3 blend films without and with thermal annealing.

TA temperature (°C)	*q* (Å^{-1})	d-spacing (Å)	FWHM Δq (Å^{-1})	CCL (Å)	Area
as cast	0.34	18.29	0.069	81.74	16
70	0.34	18.43	0.068	82.96	23
90	0.34	18.51	0.061	92.47	41
110	0.33	18.96	0.066	84.37	118
130	0.33	19.21	0.063	89.32	188
150	0.33	19.01	0.059	95.34	359
130-3	0.33	18.88	0.059	95.39	182

Table S6. (100) diffraction data in out-of-plane direction of DRTT-T:N3 blend films without and with thermal annealing.

TA temperature (°C)	*q* (Å^{-1})	d-spacing (Å)	FWHM Δq (Å^{-1})	CCL (Å)	Area
No	N/A	N/A	N/A	N/A	N/A
50	0.31	20.15	0.059	95.67	9
70	0.30	20.68	0.051	109.98	79
90	0.31	20.13	0.046	123.96	165
110	0.31	20.54	0.045	126.14	747
120	0.31	20.43	0.038	150.50	1655
130	0.31	20.50	0.032	176.14	2799
150	0.30	20.61	0.029	197.22	5785

[a] N/A denotes not available.

Table S7. (100) diffraction data in out-of-plane direction of DRTT-2T:N3 blend films without and with thermal annealing.

TA temperature (°C)	q (Å^{-1})	d-spacing (Å)	FWHM Δq (Å^{-1})	CCL (Å)	Area
No	N/A	N/A	N/A	N/A	N/A
70	0.27	22.96	0.051	111.06	29
90	0.28	22.74	0.051	110.12	126
110	0.28	22.63	0.045	124.84	436
130	0.28	22.56	0.042	134.68	648
150	0.28	22.80	0.039	144.24	896

[a] N/A denotes not available.

Table S8. (100) diffraction data in out-of-plane direction of DRTT-TT:N3 blend films without and with thermal annealing.

TA temperature (°C)	q (Å^{-1})	d-spacing (Å)	FWHM Δq (Å^{-1})	CCL (Å)	Area
No	N/A	N/A	N/A	N/A	N/A
90	0.29	21.92	0.052	108.18	20
110	0.29	21.76	0.040	141.29	259
130	0.29	21.97	0.036	157.95	1016
150	0.29	21.68	0.032	175.36	1440

[a] N/A denotes not available.

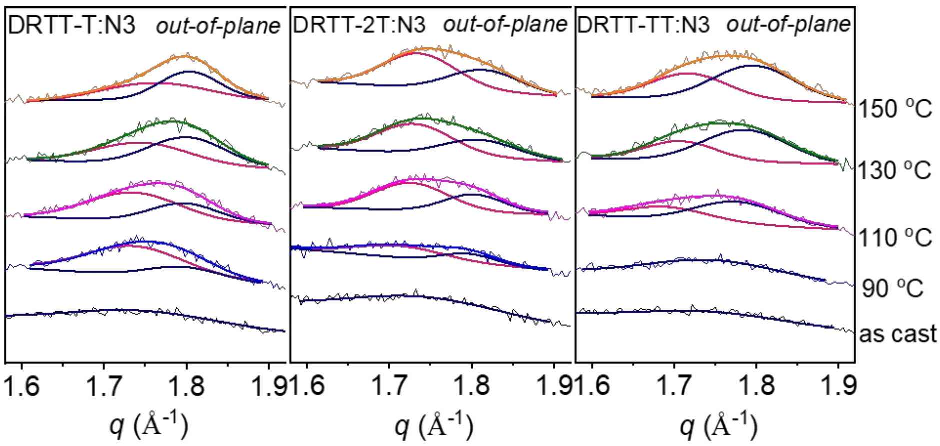

Figure S5. Multi-peaks Gaussian fitting of (010) peak in out-of-plane direction of the DRTT-T:N3, DRTT-2T:N3 and DRTT-TT:N3 blend films without and with thermal annealing.

Table S9. Multi-peaks Gaussian fitting data of (010) peaks in out-of-plane direction of DRTT-T:N3 blend films without and with thermal annealing.

TA temperature (°C)	donor					acceptor				
	q (Å^{-1})	d-spacing (Å)	FWHM Δq (Å^{-1})	CCL (Å)	Area	q (Å^{-1})	d-spacing (Å)	FWHM Δq (Å^{-1})	CCL (Å)	Area
70	1.72	3.64	0.16	35.48	22	1.80	3.49	0.12	46.18	9
90	1.74	3.62	0.14	41.11	28	1.80	3.50	0.10	54.50	9
110	1.74	3.62	0.13	43.15	27	1.80	3.49	0.10	58.51	13
130	1.75	3.60	0.13	42.36	21	1.80	3.49	0.11	51.70	23
150	1.76	3.56	0.16	34.79	23	1.80	3.48	0.09	66.42	18

Table S10. Multi-peaks Gaussian fitting data of (010) peaks in out-of-plane direction of DRTT-2T:N3 blend films without and with thermal annealing.

TA temperature (°C)	donor					acceptor				
	q (Å^{-1})	d-spacing (Å)	FWHM Δq (Å^{-1})	CCL (Å)	Area	q (Å^{-1})	d-spacing (Å)	FWHM Δq (Å^{-1})	CCL (Å)	Area
90	1.68	3.74	0.18	32.02	22	1.79	3.51	0.11	52.09	10
110	1.73	3.64	0.11	53.17	22	1.80	3.48	0.09	60.03	11
130	1.73	3.63	0.11	53.41	23	1.81	3.47	0.11	53.27	14
150	1.74	3.62	0.11	53.77	27	1.81	3.46	0.10	55.58	16

Table S11. Multi-peaks Gaussian fitting data of (010) peaks in out-of-plane direction of DRTT-TT:N3 blend films without and with thermal annealing.

TA temperature (°C)	donor					accepter				
	q (Å^{-1})	d-spacing (Å)	FWHM Δq (Å^{-1})	CCL (Å)	Area	q (Å^{-1})	d-spacing (Å)	FWHM Δq (Å^{-1})	CCL (Å)	Area
110	1.69	3.72	0.12	47.82	12	1.78	3.54	0.12	47.73	19
130	1.71	3.68	0.10	55.91	14	1.79	3.52	0.12	46.38	29
150	1.72	3.66	0.11	51.55	21	1.80	3.50	0.12	48.43	30

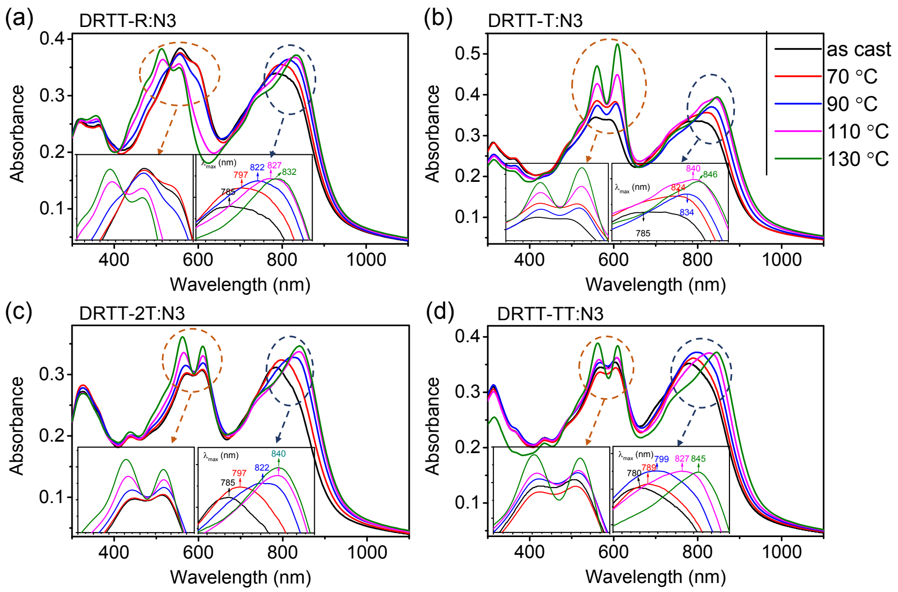

Figure S6. Absorption spectra of DRTT-R:N3 (a), DRTT-T:N3 (b), DRTT-2T:N3 (c) and DRTT-TT:N3(d) blend films without and with thermal annealing. The orange and green dashed circles are representative of the change of peak position with the increasing thermal annealing temperature of the donor and acceptor in the blend films, respectively.

Table S12. The detailed photovoltaic performance of OSCs based on DRTT-R:N3 without and with thermal annealing.

TA temperature (°C)	V_{OC} [a] (V)	J_{SC} [a] (mA·cm^{-2})	FF [a]	PCE [a] (%)
As cast	0.92 (0.92±0.00)	13.16 (12.75±0.32)	47.8 (45.7±1.7)	5.74 (5.35±0.31)
100	0.90 (0.89±0.01)	14.20 (14.14±0.08)	47.8 (46.0±1.9)	6.07 (5.80±0.27)
110	0.89 (0.89±0.00)	15.90 (14.98±0.43)	50.9 (50.0±0.7)	7.11 (6.69±0.23)
120	0.89 (0.88±0.01)	15.73 (14.96±0.45)	55.5 (52.8±1.7)	7.52 (6.98±0.40)
130	0.88 (0.88±0.00)	15.78 (15.01±0.42)	56.4 (55.4±0.9)	7.74 (7.32±0.28)
140	0.88 (0.88±0.00)	15.46 (15.00±0.28)	55.4 (54.8±1.7)	7.57 (7.23±0.33)

[a] Optimal and statistical results are listed outside of parentheses and in parentheses, respectively. The average values are obtained from over 20 devices.

Table S13. The detailed photovoltaic performance of OSCs based on DRTT-T:N3 without and with thermal annealing.

TA temperature (°C)	V_{OC} [a] (V)	J_{SC} [a] (mA·cm^{-2})	FF [a]	PCE [a] (%)
As cast	0.90 (0.90±0.00)	15.09 (14.55±0.30)	47.5 (47.2±0.7)	6.44 (6.16±0.16)
90	0.89 (0.88±0.01)	18.35 (18.02±.37)	59.7 (58.1±1.6)	9.52 (9.22±0.52)
100	0.88 (0.88±0.00)	20.68 (20.40±0.47)	64.9 (63.7±1.3)	11.84 (11.42±0.32)
110	0.87 (0.87±0.00)	20.79 (20.73±0.19)	64.8 (63.0±1.4)	11.63 (11.30±0.27)

[a] Optimal and statistical results are listed outside of parentheses and in parentheses, respectively. The average values are obtained from over 20 devices.

Table S14. The detailed photovoltaic performance of OSCs based on DRTT-2T:N3 without and with thermal annealing.

TA temperature (°C)	V_{OC} [a] (V)	J_{SC} [a] (mA·cm^{-2})	FF [a]	PCE [a] (%)
As cast	0.89 (0.89±0.00)	17.63 (17.09±0.65)	49.4 (47.3±1.4)	7.69 (7.13±0.50)
90	0.88 (0.88±0.00)	19.28 (18.60±0.60)	53.5 (51.7±1.5)	9.01 (8.44±0.51)
100	0.86 (0.86±0.00)	20.82 (20.69±0.18)	57.1 (56.7±0.8)	10.22 (10.09±0.14)
110	0.85 (0.85±0.00)	21.37 (20.91±0.21)	59.8 (58.7±0.9)	10.86 (10.44±0.22)
120	0.83 (0.83±0.00)	20.07 (19.77±0.27)	54.7 (53.4±1.1)	9.13 (8.78±0.31)

[a] Optimal and statistical results are listed outside of parentheses and in parentheses, respectively. The average values are obtained from over 20 devices.

Table S15. The detailed photovoltaic performance of OSCs based on DRTT-TT:N3 without and with thermal annealing.

TA temperature (°C)	V_{OC} [a] (V)	J_{SC} [a] (mA·cm^{-2})	FF [a]	PCE [a] (%)
As cast	0.90 (0.90±0.00)	17.13 (16.42±0.50)	48.8 (47.0±1.2)	7.46 (6.90±0.33)
100	0.90 (0.90±0.00)	17.23 (16.96±0.23)	49.5 (48.5±1.0)	7.54 (7.43±0.10)
110	0.90 (0.89±0.01)	18.10 (17.71±0.19)	49.7 (49.2±0.6)	8.01 (7.81±0.12)
120	0.88 (0.87±0.01)	19.82 (19.47±0.35)	52.6 (51.5±0.9)	9.07 (8.80±0.19)
130	0.85 (0.85±0.00)	21.12 (20.82±0.51)	55.3 (53.6±1.4)	9.91 (9.49±0.34)
140	0.82 (0.82±0.00)	19.60 (19.09±0.42)	50.2 (49.1±0.9)	8.12 (7.88±0.20)

[a] Optimal and statistical results are listed outside of parentheses and in parentheses, respectively. The average values are obtained from over 20 devices.

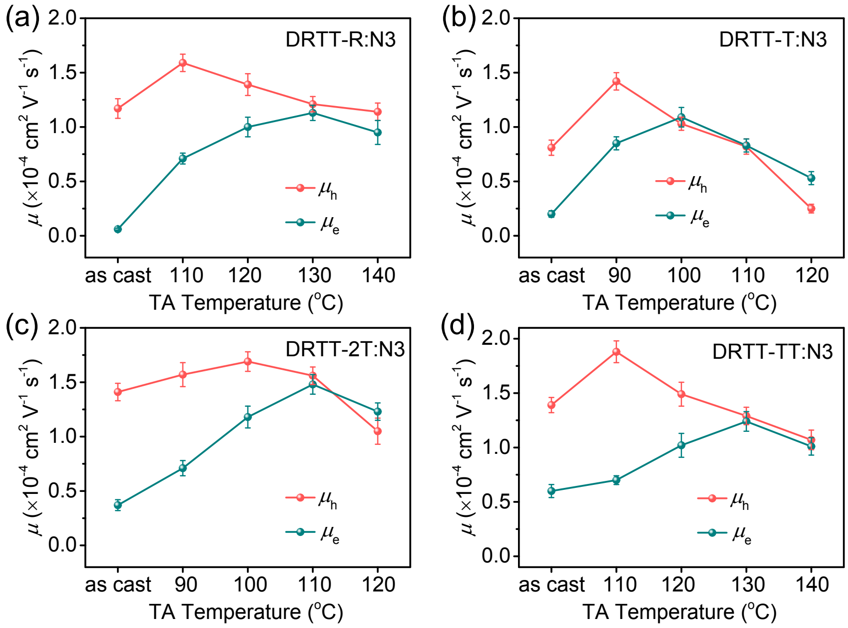

Figure S7. The hole and electron mobilities of DRTT-R:N3 (a), DRTT-T:N3 (b), DRTT-2T:N3 (c) and DRTT-TT:N3 (d) blend films as a function of TA temperature.

Table S16. Mobility results of SCLC devices based on donor:N3 blend films.

donor:N3	TA temperature (°C)	μ_e [a] (10^{-4} cm^2 V^{-1} s^{-1})	μ_h [a] (10^{-4} cm^2 V^{-1} s^{-1})
DRTT-R:N3	NO	0.07 (0.06±0.01)	1.29 (1.17±0.09)
	110	0.78 (0.71±0.05)	1.67 (1.59±0.08)
	120	1.11 (1.00±0.09)	1.51 (1.39±0.10)
	130	1.22 (1.13±0.07)	1.30 (1.21±0.07)
	140	1.07 (0.95±0.11)	1.25 (1.14±0.08)
DRTT-T:N3	NO	0.24 (0.20±0.03)	0.90 (0.81±0.07)
	90	0.92 (0.85±0.06)	1.51 (1.42±0.08)
	100	1.17 (1.09±0.09)	1.10 (1.03±0.06)
	110	0.91 (0.83±0.06)	0.91 (0.82±0.07)
	120	0.61 (0.53±0.06)	0.31 (0.25±0.04)
DRTT-2T:N3	NO	0.42 (0.37±0.05)	1.50 (1.41±0.08)
	90	0.79 (0.71±0.07)	1.70 (1.57±0.11)
	100	1.29 (1.18±0.10)	1.83 (1.69±0.09)
	110	1.60 (1.48±0.09)	1.65 (1.56±0.08)
	120	1.34 (1.23±0.08)	1.19 (1.05±0.12)
DRTT-TT:N3	NO	0.66 (0.60±0.06)	1.47 (1.39±0.07)
	110	0.75 (0.70±0.04)	1.97 (1.88±0.10)
	120	1.14 (1.02±0.11)	1.63 (1.49±0.11)
	130	1.35 (1.24±0.09)	1.38 (1.29±0.08)
	140	1.13 (1.01±0.08)	1.19 (1.07±0.09)

[a] Optimal and statistical results are listed outside of parentheses and in parentheses, respectively. The average values are obtained from over 15 devices. [b] N/A denotes not available.

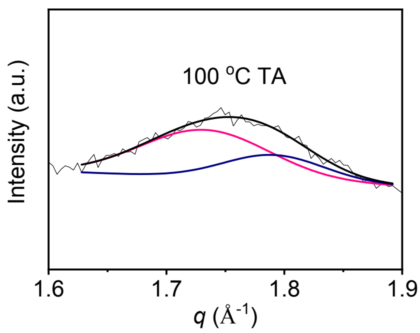

Figure S8. Multi-peaks gaussian fitting of (010) peak in out-of-plane direction of the DRTT-T:N3 blend film with thermal annealing at 100 °C.

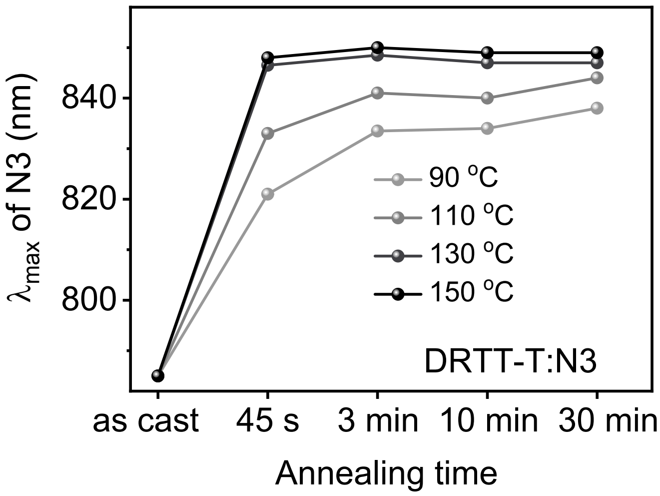

Figure S9. Absorption data (λ_{max} of N3) as a function of annealing temperature and time of DRTT-T:N3 based blend films.

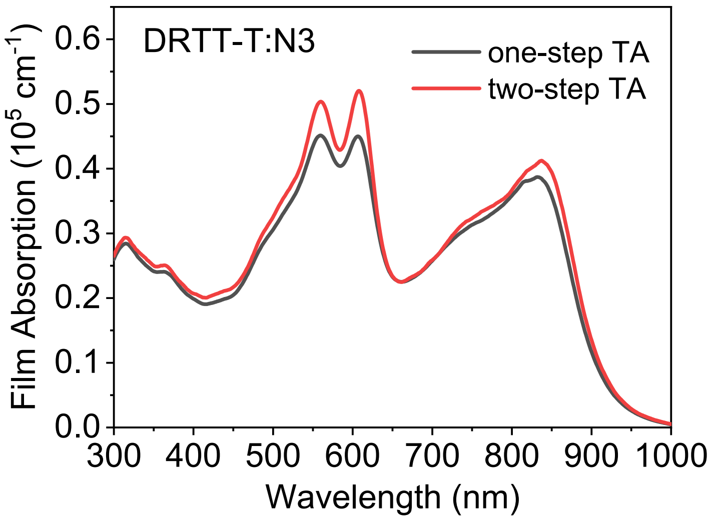

Figure S10. Absorption spectra of DRTT-T:N3 blend films with one-step and two-step thermal annealing.

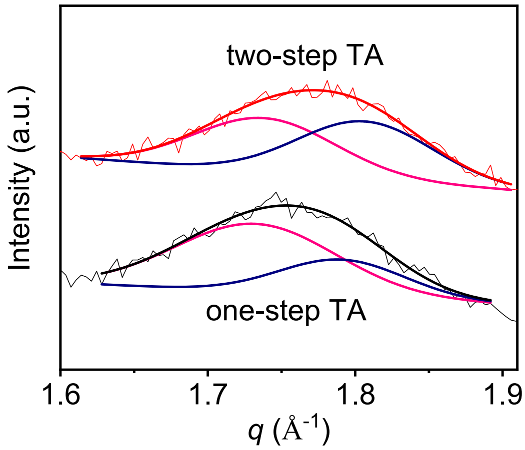

Figure S11. Multi-peaks gaussian fitting of (010) peak in out-of-plane direction of the DRTT-T:N3 blend films with one-step and two-step thermal annealing.

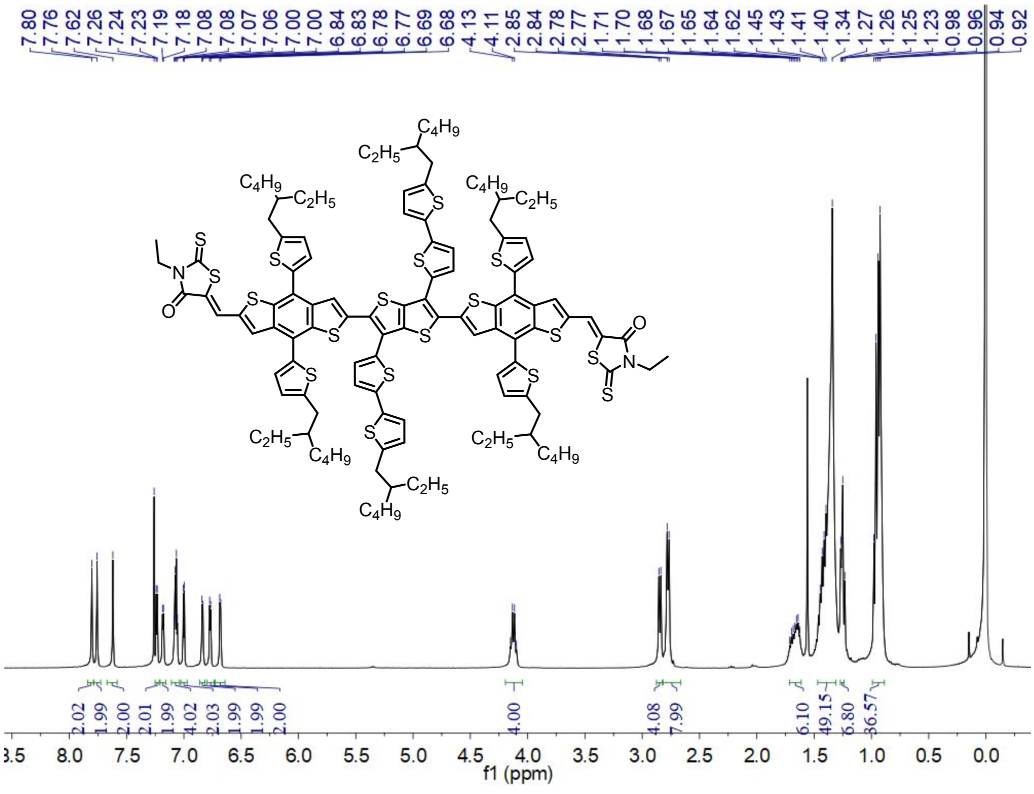

Figure S12. ^{1}H NMR spectrum of compound DRTT-2T.

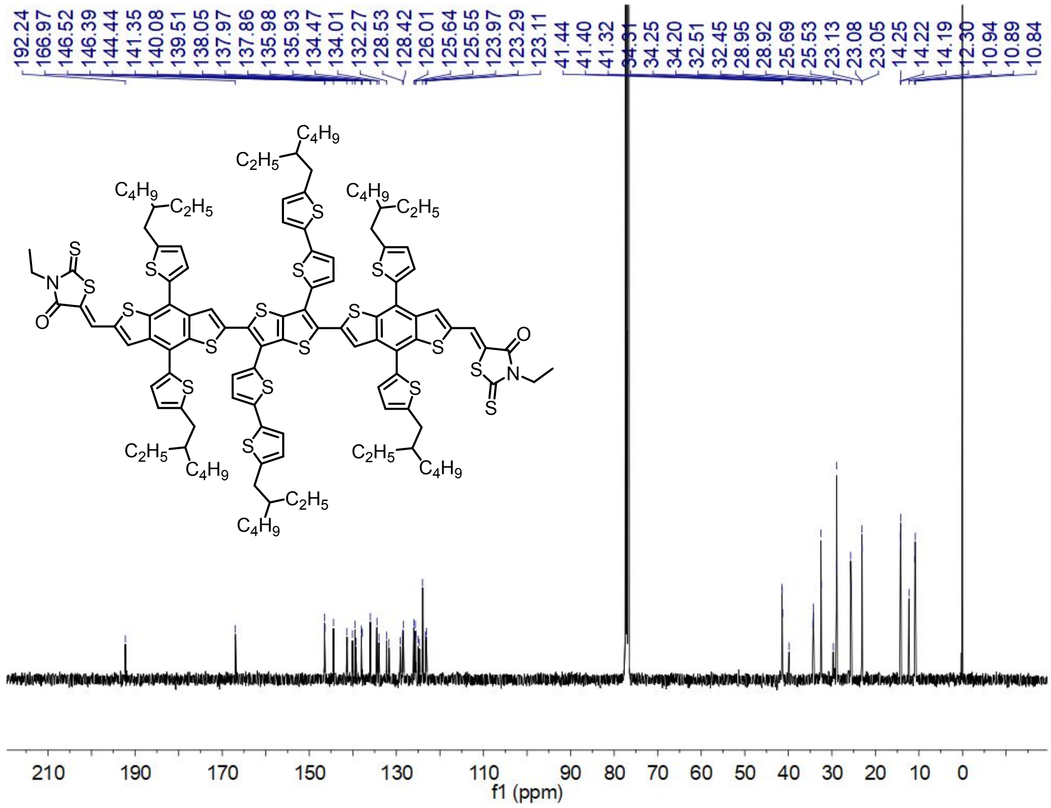

Figure S13. ^{13}C NMR spectrum of compound DRTT-2T.

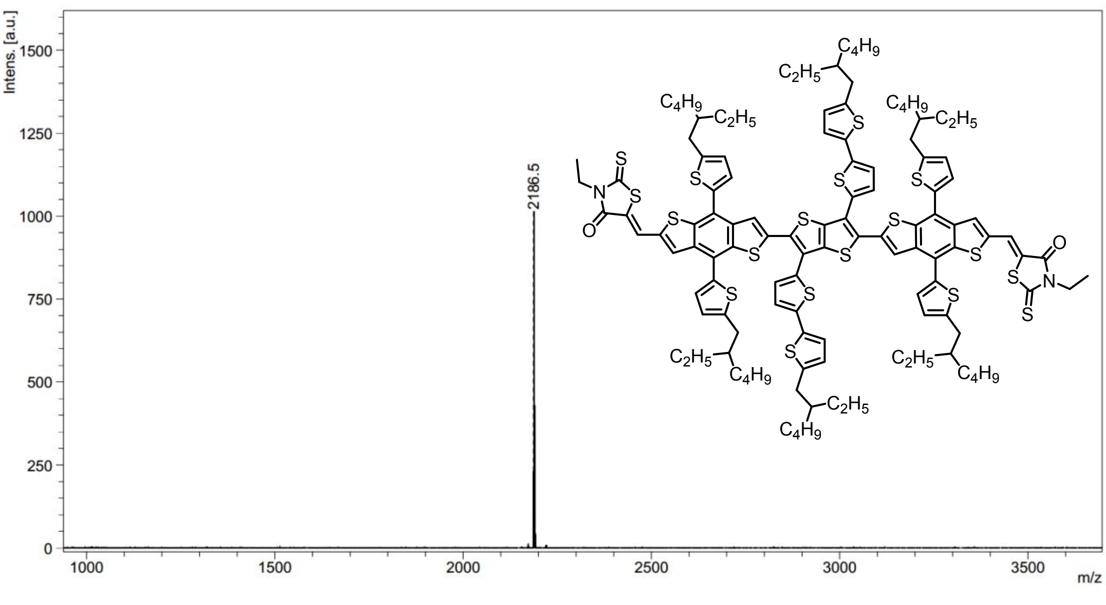

Figure S14. The MALDI-TOF mass spectrum of DRTT-2T.

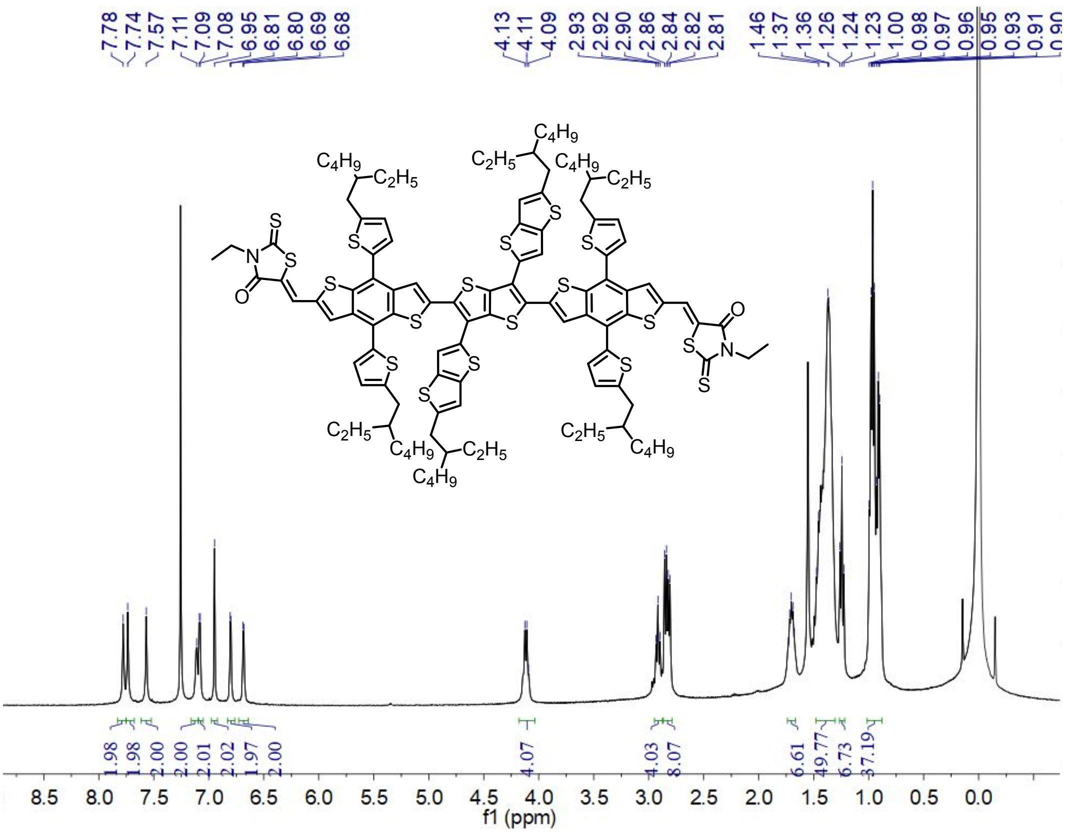

Figure S15. ^{1}H NMR spectrum of compound DRTT-TT.

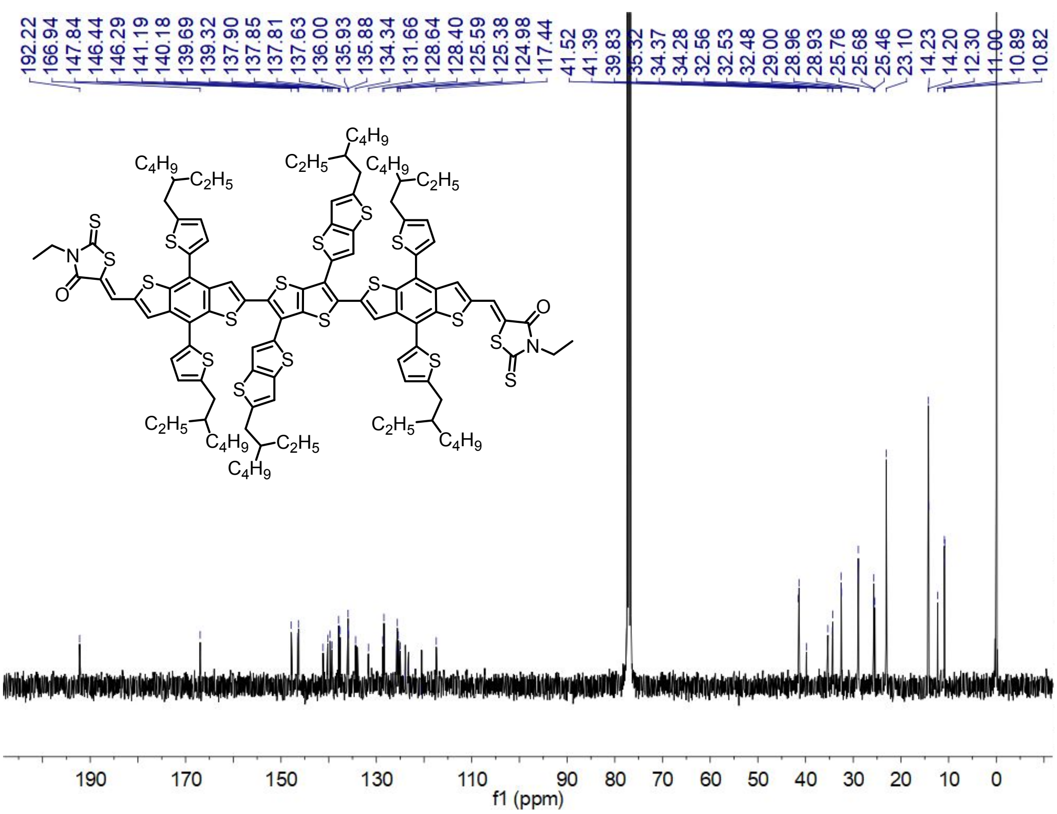

Figure S16. ^{13}C NMR spectrum of compound DRTT-TT.

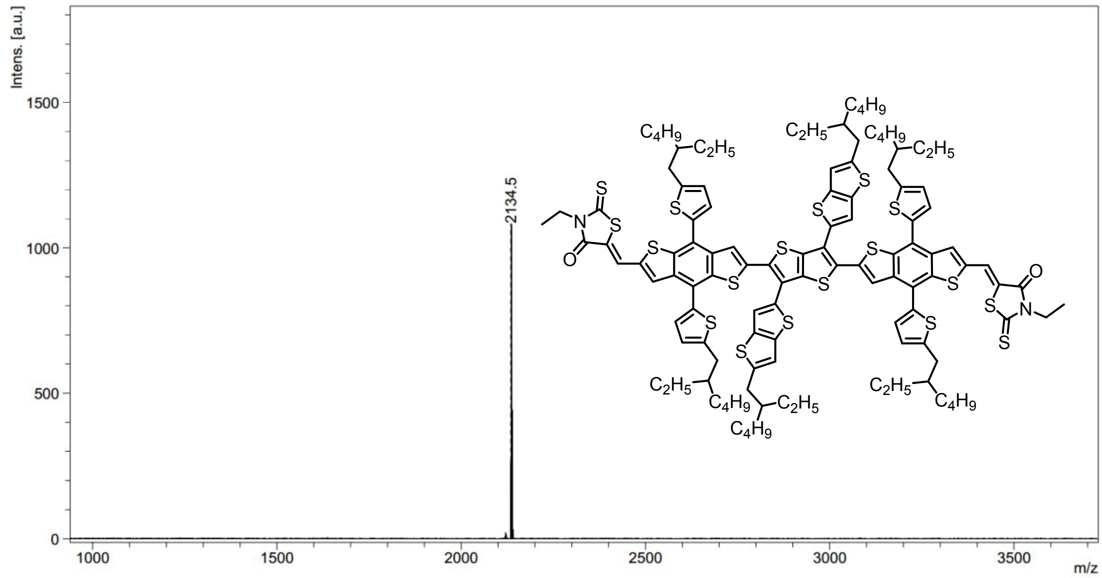

Figure S17. The MALDI-TOF mass spectrum of DRTT-TT.

5. References

1. Cheng, X.; Li, M.; Guo, Z.; Yu, J.; Lu, G.; Bu, L.; Ye, L.; Ade, H.; Chen, Y.; Geng, Y. "Twisted" conjugated molecules as donor materials for efficient all-small-molecule organic solar cells processed with tetrahydrofuran. *J. Mater. Chem. A* **2019,** *7*, 23008-23018.

2. Zhou, J.; Zuo, Y.; Wan, X.; Long, G.; Zhang, Q.; Ni, W.; Liu, Y.; Li, Z.; He, G.; Li, C.; Kan, B.; Li, M.; Chen, Y. Solution-processed and high-performance organic solar cells using small molecules with a benzodithiophene unit. *J. Am. Chem. Soc.* **2013,** *135*, 8484-8487.

3. Kim, J.-H.; Song, C. E.; Kim, B.; Kang, I.-N.; Shin, W. S.; Hwang, D.-H. Thieno[3,2-b]thiophene-Substituted Benzo[1,2-b:4,5-b′]dithiophene as a Promising Building Block for Low Bandgap Semiconducting Polymers for High-Performance Single and Tandem Organic Photovoltaic Cells. *Chem. Mater.* **2014,** *26*, 1234-1242.

4. Yang, L.; Zhang, S.; He, C.; Zhang, J.; Yao, H.; Yang, Y.; Zhang, Y.; Zhao, W.; Hou, J. New Wide Band Gap Donor for Efficient Fullerene-Free All-Small-Molecule Organic Solar Cells. *J. Am. Chem. Soc.* **2017,** *139*, 1958-1966.